Biomech Model Mechanobiol (2009) 8:337–343
DOI 10.1007/s10237-009-0150-9

ORIGINAL PAPER

A novel model-gel-tissue assay analysis for comparing tumor elastic properties to collagen content

Stephanie L. Barnes · Pampee P. Young · Michael I. Miga

Received: 24 September 2008 / Accepted: 23 February 2009 / Published online: 24 March 2009

Abstract In previous work, a new assay was realized for determining soft-tissue mechanical properties. The method, named the model-gel-tissue (MGT) assay, couples material testing with a finite element model built from a micro-CT image acquisition of a gel-embedded tissue specimen to determine its mechanical properties. Given recent reports demonstrating that increased stromal collagen promotes mammary tumor initiation and proliferation, in this paper, the MGT assay is used to evaluate the modulus of murine mammary tumors and is subsequently correlated quantitatively to type I collagen content. In addition, preliminary testing of the assay sensitivity with respect to gel-volume to tissue-mass ratio is reported here. The results demonstrate a strong linear correlation between tumor mechanical properties and collagen content ($R^2 = 0.9462$). This result is important because mechanical stiffness as provided by the MGT assay is very similar to parameters under clinical investigation using elastographic imaging techniques. The sensitivity tests indicated that an approximate gel-volume to tissue-mass ratio threshold of 16.5 ml g^{-1} is needed for successful analysis. This is an important result in that it presents guideline constraints for conducting this analysis.

Keywords Finite element modeling · Murine mammary tumor · Elastic modulus · Mechanical testing

S. L. Barnes · M. I. Miga (✉)
Department of Biomedical Engineering, Vanderbilt University, 5824 Stevenson Center, Nashville, TN 37235, USA
e-mail: michael.i.miga@vanderbilt.edu

S. L. Barnes
e-mail: steph.barnes@vanderbilt.edu

P. P. Young
Department of Pathology, Vanderbilt University School of Medicine, C-3321 A Medical Center North, 1161 21st Avenue South, Nashville, TN 37232, USA

P. P. Young
The Department of Veterans Affairs Medical Center, Nashville, TN, USA

M. I. Miga
Department of Radiology and Radiological Sciences, Vanderbilt University Medical Center, Nashville, TN 37232, USA

M. I. Miga
Vanderbilt University Medical Center, Vanderbilt University Institute of Imaging Science, 1161 21st Avenue South Medical Center North, AA-1105, Nashville, TN 37232, USA

1 Introduction

Assessment of tissue stiffness often plays an integral role in research and clinical diagnostics since it has been identified as an indicator of a variety of pathological conditions, including hepatic fibrosis, arterial disease, myocardial infarction, breast cancer, prostatic cancer, thyroid disease, and skin cancer, among others (Anderson 1980; Covell and Ross 1973; de Ledinghen et al. 2006; Diamond and Forrester 1972; Gaasch et al. 1976; Giannattasio and Mancia 2002; Herrington et al. 2004; Krouskop et al. 1998; Levy et al. 2001; Nagasaki et al. 2006; Phipps et al. 2005; Tilleman et al. 2004; vanPopele et al. 2001; Yeh et al. 2002; Ziol et al. 2005). In addition, recently developed medical imaging modalities are attempting to render non-invasive measurements of these properties for disease screening (commonly cancer screening) and therapeutic applications (Bilgen et al. 2003; Fahey et al. 2008; Garra et al. 1997; Muthupillai et al. 1995; Ophir et al. 1991; Sandrin et al. 2003; Sinkus et al. 2008; Souchon et al. 2003; Venkatesh et al. 2008). However, direct mechanical measurement of tissue for modulus assessment and method validation has proven difficult due to the inherent irregular tissue shape and the challenge of preparing

tissue samples for traditional mechanical testing methods. Some material testing methods have been developed that are applicable to a specific tissue configuration; for example, indentation testing for layered slab tissues. While a very common approach, the determination of elastic properties from this data is often based on certain geometric shapes and boundary conditions. In the case of tissue resection and biopsy specimens, which are generally the gold-standard pathological sampling techniques, the tissue samples would routinely violate many of these assumptions. Thus, the development of a mechanical property assessment technique that can be adaptable to the uncertainty of tissue size and shape and yet be quantitative would be an important contribution toward understanding biomarkers associated with tissue structure.

With respect to the macroscopic determination of mechanical properties, the two primary protein components that define mechanical stability of soft tissue are collagen and elastin. These proteins directly influence the structural integrity of tissue, and an assessment of the amount of collagen in a sample is a measure that reflects the load-bearing nature of tissue, and hence its stiffness. Changes to tissue health can lead to altered distributions of these particular proteins within soft tissue (Buckley et al. 1988). For example, in recent reports increased stromal collagen has been shown to increase tumor formation and proliferation in murine mammary tissue by threefold and has resulted in a more invasive phenotype with increased metastasis (Provenzano et al. 2008). The possibility of using an assessment of collagen to predict tumorigenic behavior is intriguing, but the interaction and change to the relationship between cellular structure and modulus in the diseased state is to some degree uncertain, and its relationship at clinically relevant diagnostic length scales is equally uncertain. The standard method used for collagen assessment is histological analysis; however, at best histological processing provides an indirect relationship to collagen's functional mechanical role, and it is this functional role that is critical in many ways to the use of mechanical properties as a biomarker. For example, breast cancer and liver fibrosis are often detected by palpation (Ghany and Doo 2005; Mahoney and Csima 1982; McCormick and Nolan 2004; Naylor 1994). Other areas of study such as fracture repair and wound healing are also characterized by mechanical performance (Campos et al. 2008; Delos et al. 2008; Gal et al. 2006; Huddleston et al. 2000; Shefelbine et al. 2005). While these are important areas, it would also be interesting to extrapolate the role that mechanical properties or the monitoring of tissue architecture could play in cancer evaluation.

In this work, an ex vivo mechanical testing assay that was previously reported is used within the context of measuring mechanical properties of arbitrarily shaped tissue volumes from a murine mammary tumor model. The assay involves suspending freshly excised tissue specimen within a rapidly congealing gel, imaging the sample, evaluating mechanical performance using standard material testing equipment, and then implementing a model-fitting process for modulus assessment. The assay is called the model-gel-tissue (MGT) assay, and is used here to demonstrate the link between tissue mechanical properties and collagen content for mammary tumors. Preliminary work utilizing the assay within a liver fibrosis murine model has been reported (Barnes et al. 2007). In this work, the utility of the assay to evaluate various tissue types is demonstrated, as a shift is made from fibrotic liver to mammary tumor tissue. This expansion of the assay analysis to other tissue types, in particular cancer-based, begins to provide a more quantitative understanding of the stiffness biomarker that is commonly used to detect breast cancer. In addition, the work presented here is concerned with the specific task of linking structural load-bearing changes to a histological assessment of a murine breast cancer system. In doing so, a critical quantitative correlation to cellular microstructural content, which had not been realized in the previous work, is demonstrated. In addition to this considerable advance, the tissue specimen volume has been reduced by one order of magnitude such that it is now biopsy-relevant and a preliminary sensitivity study regarding gel-volume to tissue-mass ratio is explored.

2 Materials and methods

The work reported herein concerns the analysis of the modulus of elasticity of nine murine mammary tumors as measured by the MGT assay previously reported. The mouse model was prepared with 1×10^6 murine breast cancer cells derived from mouse mammary tumor virus polyomavirus middle T transgenic lines (PyV-mT; maintained in DMEM, 10% FCS, 5.0 ng ml^{-1} 17-β estradiol, 1 µg ml^{-1} progesterone), which were implanted contralaterally in FVB/nJ host mice in the 4th mammary fat pad. Tumor tissues were collected after 30–40 days, which allotted growth to approximately 200 mm^3, and sectioned for analysis. The largest section was utilized for modulus evaluation in the MGT assay. Collagen content of the tumors was determined from the acid-hydrolyzed homogenate of a separate tumor segment. Amino-acid analysis of the derivatized hydrolyzate yielded hydroxyproline and other amino acids to estimate both total and relative collagen content (Buckley et al. 1988). This value was then used as a comparison for our MGT assay evaluation of the tissue modulus. These tests were prepared in a blinded fashion from the MGT assay and were only available post MGT assay conclusion. In addition, a histological analysis was performed on tissue samples in order to ensure that the collagen present was predominantly type I. Tissue samples underwent standard immunohistological analysis,

using rabbit anti-collagen I (abcam, Cambridge, MA), which has shown 100% specificity to collagen type I and less than 1% reactivity to other collagen types. The Dako Envision+ System, DAB/Peroxidase (DakoCytomation) was used to produce localized, visible staining of the collagen. For comparison purposes, adjacent sections of tumor were stained with Masson's Trichrome to visualize extracellular collagen deposition.

The previously developed MGT assay was used in this work to measure the mechanical properties of the murine mammary tumor tissue samples. The assay combines finite element modeling of the gel-tissue composite with direct mechanical testing to evaluate the mechanical properties of the tissue sample. An outline of the assay is depicted below (Fig. 1).

Implementation of the MGT assay system required production of a uniform gel with embedded tissue sample as well as rigorously defined material testing protocols. The gel that proved most amenable to the demands of the system was a rapidly congealing polyacrylamide (PA) gel. The components of such a gel were 1 molar Tris buffer, 10% ammonium persulfate (APS) solution, and 30% acrylamide/polyacrylamide (Bio-Rad Laboratories). Since multiple samples could be generated during the course of one experiment, an initial solution was generated for use in all gel generations. For this research, a 4.5% PA gel, which had a modulus of approximately 2.5 kPa, was utilized. It is necessary for the MGT assay that the modulus of the gel be similar to that expected for the tissue; if the gel is too stiff, the incremental effect of the tissue modulus on the composite system is undetectable. In addition, the ratio of gel-volume to tissue-mass proved pivotal in the effectiveness of the assay. In an attempt to compensate for the varying tumor tissue volumes across samples, we gradually varied the gel volume, resulting in gel-volume to tissue-mass ratios ranging from 4.43 to 32.68. The success of the assay appears to be linked to this ratio (Table 1). Based on this preliminary analysis, a volume of 1.4 ml of solution was generally used; however, this amount could be varied dependent on the tissue mass if necessary. With respect to setup, the diameter of the gel cylinder could be varied to accommodate different tissue shapes, but it was necessary that the gel completely envelop the tissue for the assay evaluation. In the mammary tumor case, well plates with a diameter of 16 mm proved sufficient for the extracted tissue size. To generate the gels, the desired volume of buffer/APS/PA solution was added to one of the wells. In addition, to provide a distinguishable boundary between the tissue and the gel in CT scans for the purpose of extracting the geometric shape for modeling (i.e. image segmentation), Optiray (Mallinckrodt Inc.), a CT contrast agent, was added to the mixture. The tissue was then suspended in the liquid using forceps while the polymerization initiator, TEMED, was added to the well. Solidification of the gel was complete in approximately 2 min. In addition to the embedded tissue

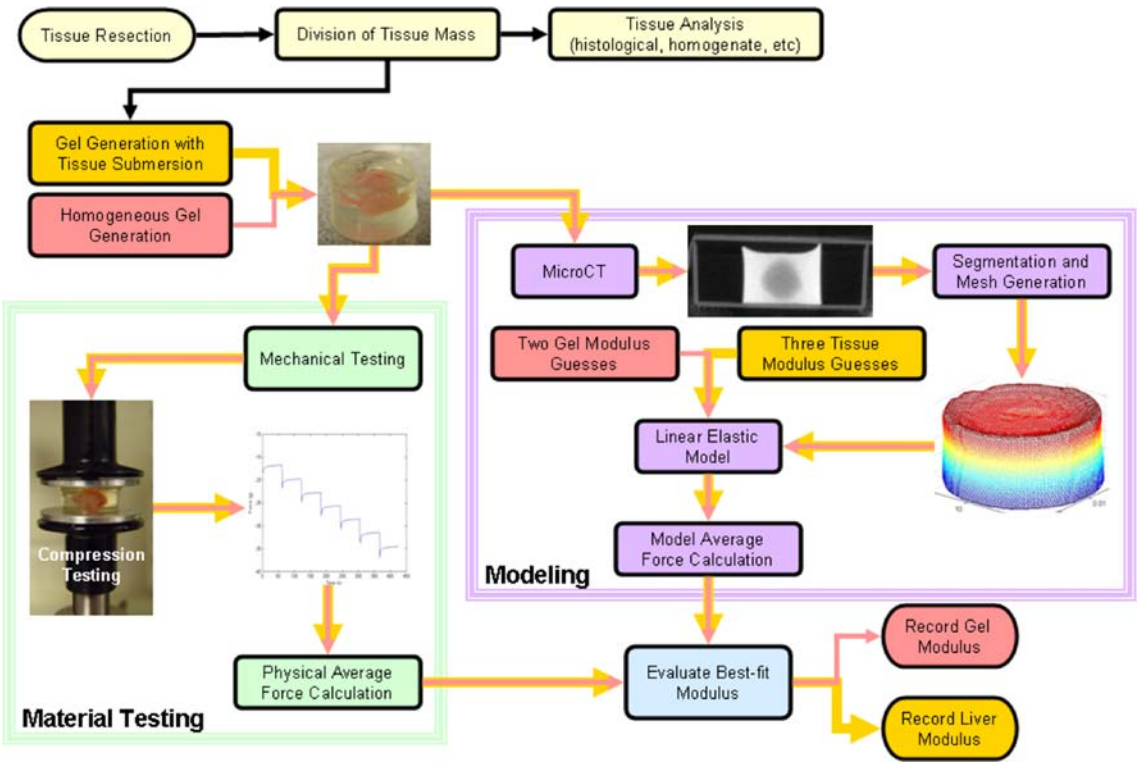

Fig. 1 Assay outline

Table 1 Gel-volume to tissue-mass ratio

Mammary tumor mass (g)	Gel volume (ml)	Gel-to-tissue ratio (ml g^{-1})	Positive analysis?
0.3819	2	5.24	Yes
0.3580	2	5.59	Yes
0.4519	2	4.43	Yes
0.1057	2	18.92	No
0.0684	2	29.24	No
0.0912	1.5	16.45	Yes
0.0950	1.5	15.79	Yes
0.0459	1.5	32.68	No
0.1011	1.4	13.85	Yes
0.2221	1.4	6.30	Yes
0.1335	1.4	10.47	Yes
0.2554	1.4	5.48	Yes

gels, a homogeneous gel was generated at the same time for the purpose of estimating the mechanical properties of the gel itself. The homogenous gel was created following the same guidelines previously described, without suspension of the tissue. If multiple gel volumes were used in the experimentation, a homogeneous gel was generated for each volume instance.

After gel generation, the gel-tissue specimen was subjected to compression testing using the Enduratec Electroforce 3100 material tester (Bose, Enduratec Systems Group) with both force and displacement being acquired. Due to the small size of the samples, a 50-gm force transducer was utilized. The mechanical test consisted of a series of incremental unconfined step compressions to specified displacement levels, from 0.35 to 0.65 mm in 0.05 mm increments, followed by a 60-s dwell period which was implemented to dissipate the majority of the viscoelastic behavior of the tissue and gel. The compression testing was repeated twice for each gel sample. The unconfined nature of the compression was achieved experimentally by applying a lubricant to both the top and bottom platens. After material testing, the gel-tissue sample was imaged using the Imtek microCAT II scanner (Concord/CTI). Image segmentation of the CT images was performed using AnalyzeAVW (Mayo Foundation for Medical Education and Research). Upon completion of the segmentation, a surface description was generated and used as a bounding description for a custom-built tetrahedral mesh generator (Sullivan et al. 1997).

After imaging and material testing was completed, the MGT assay modulus evaluation process took place in two steps. First, the homogenous gel sample was evaluated to determine its modulus. The finite element model generated for the homogeneous gel was subjected to boundary conditions that matched the unconfined mechanical compression of the physical gel. Specifically, the top surface was subjected to a fixed normal displacement (Dirichlet boundary conditions) while being allowed to slip laterally (Neumann boundary conditions). The bottom surface of the gel experienced similar boundary conditions, with the difference being that the normal displacement was maintained at a constant zero value. Approximately ten nodes in the center of both the top and the bottom surfaces were confined laterally in order to ensure uniqueness of the computational solution. A modulus value was assumed for the gel in the model, and a forward evaluation of the displacements was calculated. From the displacement field, equivalent surface stress due to the specified compression level could be reconstructed. The resulting model stress was then converted to a force value based on the surface area of the specific gel and compared to the acquired force from the mechanical tester; the input gel modulus was varied until the model-calculated force value matched the measured force value, at which point the reference gel modulus was recorded. This value was then assumed to be the gel modulus in the gel-tissue sample evaluation. The method of tissue modulus estimation consisted of compressing the composite model according to the same mechanical testing conditions as in the homogeneous case. Three tissue modulus values were assumed within the model of the composite system and the corresponding force values were calculated. A polynomial fit was established relating tissue modulus to model-calculated force values, and the final tissue modulus was assigned based on location of the minimum difference between the modeled and measured force values.

3 Results

The results of the volume regulation testing are presented in Table 1, wherein the ratio of PA gel-volume to tumor tissue-mass is correlated to whether the MGT assay was able to successfully analyze the tissue modulus. A successful analysis was considered to be the case where a modulus value could be evaluated for the tissue. An unsuccessful analysis was defined by an inability to differentiate the specimen from the background gel due to undetectable differential force resolution experienced when adjusting the tissue modulus. In cases where the gel-volume to tissue-mass ratio is approximately 16.5 or less the assay is able to successfully evaluate the tissue modulus. According to the available data, the maximum value at which the assay is no longer able to evaluate the tissue modulus is 18.92.

The results from our murine tumor tissue assay analysis are compiled in Table 2. The first column is the tumor number given for identification purposes. The second column of the table is the modulus value as calculated by the MGT assay, and the third column is the collagen percentage as evaluated by acid-hydrolyzed homogenate analysis. A pictorial depiction of the data from Table 2 follows, wherein

Table 2 Assay and acid-hydrolyzed homogenate results

Tumor number	Modulus (Pa)	Collagen percentage
1	750	7.93
2	970	9.00
3	3,840	33.48
4	2,430	16.64
5	1,050	11.76
6	2,730	20.11
7	1,840	16.37
8	890	7.07
9	650	4.49

collagen percentage of the tumors is plotted versus the MGT assay modulus assessment for each tumor (Fig. 2). A linear regression was performed on the data, resulting in a correlation coefficient that demonstrates a strong linear correlation between the two variables ($R^2 = 0.9462$). In addition, two sets of predictive intervals (90 and 95%) are shown. These predictive intervals indicate the range of obtainable collagen percentage values correlating to a specific modulus value in future evaluations (Hines and Montgomery 1990; Montgomery and Runger 2003). In other words, these intervals depict the specificity of our assay in evaluating a correlation between the model modulus value and the analysis of collagen percentage.

Results from the histological analysis of the mammary tumor tissue are shown in Figs. 3 and 4. Representative images at 10× and 20× magnification are shown for both the immunohistological analysis for collagen type I (Fig. 3) and the Masson's trichrome staining of adjacent slices (Fig. 4). In Fig. 3, the slides were lightly counterstained with Mayer's hematoxylin to tag collagen I with a slight brown color. In Fig. 4, the light pink areas are cellular cytoplasm, while the darker pink/brown areas are the nuclear component. Blue areas in Fig. 4 are extracellular collagen. Comparison of the brown-stained collagen type I (Fig. 3) to the blue-stained ECM collagen (Fig. 4) indicates that most, if not all, of the collagen present in the tumor tissue is type I.

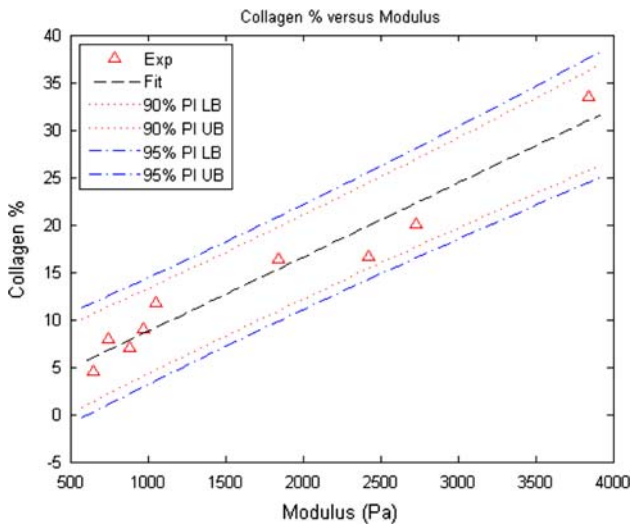

Fig. 2 Collagen percentage as a function of tumor modulus

4 Discussion

One of the aims of this work was to demonstrate that the analytic capability of the MGT assay was not limited to a specific tissue type. To this avail, murine mammary tumor tissue was used, which, by dictation of the system, is a much smaller tissue volume than the murine liver. Thus, while we were able to show the applicability of the assay to other tissue types, this work also provided insight to the required assay parameters for tissue assessment using the MGT assay; namely, the required control of the gel-volume to tissue-mass ratio. In practice, the gel must completely surround the tissue. However, if the gel volume exceeds the tissue mass by too large a ratio, the gel mechanics will overwhelm the changes to the composite mechanics and the assay will be less sensitive to contributions from the soft tissue. The realization of this volume regulation is evident from the data (Table 1). From this data, a threshold of the ratio is observed, above which the assay is not able to identify the tissue among the gel, which is important to recognize in order to ensure the fidelity of the assay. In cases where the gel-volume to tissue-mass ratio is approximately 16.5 or less the assay is able to successfully evaluate the tissue modulus. The implications are that since the tissue mass can only be minimally controlled (e.g. volume of the biopsy), control of the assay must be performed by modifying the gel recipe based on the measured mass of the resected tissue. While this is an important result, the analysis was preliminary, and the need remains to conduct a more detailed gel-volume to tissue-mass ratio sensitivity study with controlled specimen stiffness and volumes, which may provide more information regarding resolution of the assay and quite possibly an optimal ratio.

With respect to cancer screening, a common clinical presentation is a change in the mechanical stiffness of tissue in a focal region such that it becomes more rigid (e.g. breast cancer). While for conditions such as liver fibrosis, the mechanism for altered mechanical properties is well understood, this process in cancer is mechanistically unclear. As more information is uncovered regarding microstructural effects relating to tumorigenesis, such as that relating increased stromal collagen content to tumor formation and proliferation (Provenzano et al. 2008), the need to understand the underlying link between structure and function is enhanced. Our

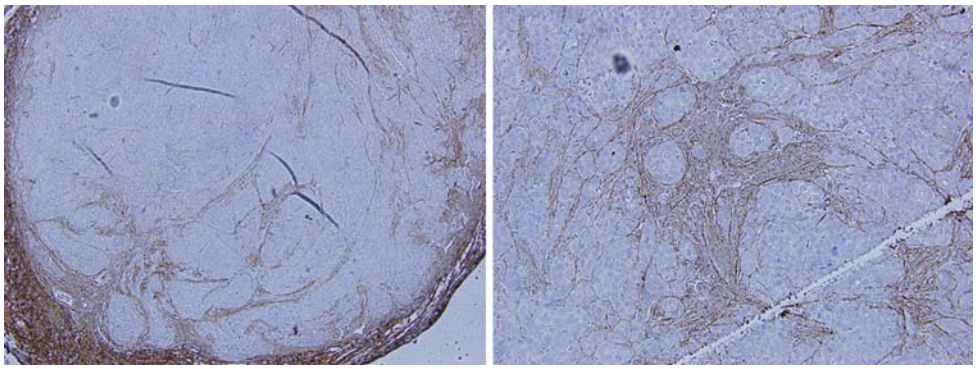

Fig. 3 Representative slice from immunohistological analysis of murine mammary tumor tissue. The two images are the same slice, with the *left* being at 10× magnification and the *right* at 20× magnification

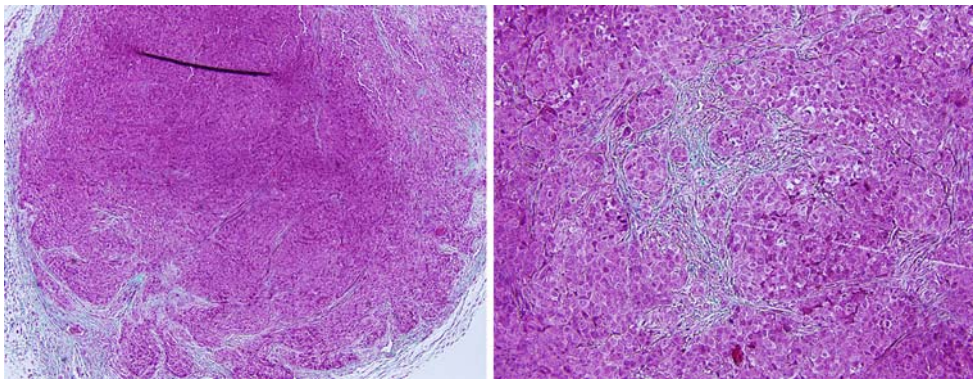

Fig. 4 Representative slice from Masson's Trichrome staining of murine mammary tumor tissue. The two images are the same slice, with the *left* being at 10× magnification and the *right* at 20× magnification

work demonstrates a distinct tracking of mechanical properties with respect to collagen content within this particular cancer model (Fig. 2). In addition, the immunohistological analysis performed indicates that the collagen content evaluated by the acid-hydrolyzed homogenate is representative of collagen type I. It is unclear if the apparent linear relationship will translate to other tumors or whether various cellular and molecular challenges will change this correlation. From a methodological standpoint, the breakthrough that the MGT assay makes is the ability to analyze mechanical properties of small animal tissue immediately postmortem while allowing the sample size to be arbitrarily shaped and very small in volume. From the clinical standpoint, the breakthrough is twofold: (1) human biopsies are generally small and arbitrarily shaped, and hence the assay could presumably be utilized in biopsy evaluation, and (2) it is clear that the MGT assay combined with other cellular assays allows more detailed understanding of the elasticity signal commonly collected by clinical elastographic imaging methods, i.e. it illuminates the relationship between the cellular biomarker of collagen presentation and the mechanical abnormalities of the tumor at the macroscopic scale.

While the general behavior reported can be intuited, the contribution is in the absolute quantification—a definable metric to relate function to histological presence. In addition, it is interesting to begin to speculate how this type of analysis can be furthered. For example, the force–displacement data for this assay was fit to a linearly elastic homogeneous computer model of the tumor. Time-varying changes were factored from the experiment by allowing sufficient time lapses to allow for a quasi-steady state force–displacement response. The reality is that these temporal behaviors have information regarding soft-tissue interstitial fluid dynamics and cell-to-cell mechanics. With more sophisticated models, and more sophisticated fitting procedures, other information regarding structure and function could possibly be determined. In addition to generating models to correlate the slow-varying transients, other altered material testing profiles could be utilized. For example, viscoelastic properties are often illuminated by testing specimens with cyclic loading; it would be interesting to put a mechanical excitation spectrum though the specimen and correlate the findings with very complex models. Another area that awaits further investigation is the enhancement of the imaging aspect to this experiment. Here, micro-CT was used to essentially capture the shape of the tissue specimen. One could envision using high-field MR techniques to get at the more fine structural heterogeneity; or perhaps, diffusion imaging could be used to highlight regions of the tumor that do not permit the traffic of interstitial fluid as readily. The ultimate triumvirate for relating structure to assessable modulus would be to combine structure-enhancing imaging sequences, sophisticated testing regiments, and detailed cell and molecular assays. The MGT assay is a first move in this direction.

References

Anderson W (1980) Synopsis of pathology. Mosby, St. Louis

Barnes SL, Lyshchik A, Washington MK, Gore JC, Miga MI (2007) Development of a mechanical testing assay for fibrotic murine liver. Med Phys 34:4439–4450. doi:10.1118/1.2795665

Bilgen M, Srinivasan S, Lachman LB, Ophir J (2003) Elastography imaging of small animal oncology models: a feasibility study. Ultrasound Med Biol 29:1291–1296. doi:10.1016/S0301-5629(03)01013-5

Buckley A, Hill KE, Davidson JM (1988) Collagen metabolism. Methods Enzymol: 674–694. doi:10.1016/0076-6879(88)63056-4

Campos AC, Groth AK, Branco AB (2008) Assessment and nutritional aspects of wound healing. Curr Opin Clin Nutr Metab Care 11:281–288. doi:10.1097/MCO.0b013e3282fbd35a

Covell JW, Ross JJ (1973) Nature and significance of alterations in myocardial compliance. Am J Cardiol 32:449–455. doi:10.1016/S0002-9149(73)80035-9

de Ledinghen V, Douvin C, Kettaneh A, Ziol M, Roulot D, Marcellin P, Dhumeaux D, Beaugrand M (2006) Diagnosis of hepatic fibrosis and cirrhosis by transient elastography in hiv/hepatitis c virus-coinfected patients. J Acquir Immune Defic Syndr 41:175–179. doi:10.1097/01.qai.0000194238.15831.c7

Delos D, Yang X, Ricciardi BF, Myers ER, Bostrom MPG, Camacho NP (2008) The effects of rankl inhibition on fracture healing and bone strength in a mouse model of osteogenesis imperfecta. J Orthop Res 26:153–164. doi:10.1002/jor.20469

Diamond G, Forrester JS (1972) Effect of coronary artery disease and acute myocardial infarction on left ventricular compliance in man. Circulation 45:11–19

Fahey BJ, Nelson RC, Bradway DP, Hsu SJ, Dumont DM, Trahey GE (2008) In vivo visualization of abdominal malignancies with acoustic radiation force elastography. Phys Med Biol 53:279–293. doi:10.1088/0031-9155/53/1/020

Gaasch WH, Levine HJ, Quinones MA, Alexander JK (1976) Left ventricular compliance: mechanisms and clinical implications. Am J Cardiol 38:645–653. doi:10.1016/S0002-9149(76)80015-X

Gal P, Toporcer T, Vidinsky B, Mokry M, Novotny M, Kilik R, Smetana K, Gal T, Sabo J (2006) Early changes in the tensile strength and morphology of primary sutured skin wounds in rats. Folia Biol 52:109–115

Garra BS, Cespedes I, Ophir J, Spratt SR, Zuurbier RA, Magnant CM, Pennanen MF (1997) Elastography of breast lesions: intial clinical results. Radiology 202:79–86

Ghany M, Doo E (2005) Assessment of liver fibrosis: Palpate, poke, or pulse? Hepatology 42:759–761. doi:10.1002/hep.20913

Giannattasio C, Mancia G (2002) Arterial distensibility in humans. Modulating mechanisms, alterations in diseases and effects of treatment. J Hypertens 20:1889–1899. doi:10.1097/00004872-200210000-00001

Herrington DM, Brown WV, Mosca L, Davis W, Eggleston B, Hundley WG, Raines J (2004) Relationship between arterial stiffness and subclinical aortic atherosclerosis. Circulation 110:432–437. doi:10.1161/01.CIR.0000136582.33493.CC

Hines WW, Montgomery DC (1990) Probability and statistics in engineering and management science. Wiley, New York

Huddleston PM, Steckelberg JM, Hanssen AD, Rouse MS, Bolander ME, Patel R (2000) Ciprofloxacin inhibition of experimental fracture-healing. J Bone Jt Surg 82:161–173

Krouskop TA, Wheeler TM, Kallel F, Garra BS, Hall T (1998) Elastic moduli of breast and prostate tissues under compression. Ultrason Imaging 20:260–274

Levy M, Bass H, Stren R (2001) Handbook of elastic properties of solids, liquids, and gases. Academic Press, San Diego

Mahoney L, Csima A (1982) Efficiency of palpation in clinical detection of breast cancer. Can Med Assoc J 127:729–730

McCormick P, Nolan N (2004) Palpable epigastric liver as a physical sign of cirrhosis: a prospective study. Eur J Gastroenterol Hepatol 16:1331–1334. doi:10.1097/00042737-200412000-00016

Montgomery DC, Runger GC (2003) Applied statistics and probability for engineers. Wiley, New York

Muthupillai R, Lomas DJ, Rossman PJ, Greenleaf JF, Manduca A, Ehman RL (1995) Magnetic-resonance elastography by direct visualization of propagating acoustic strain waves. Science 269:1854–1857. doi:10.1126/science.7569924

Nagasaki T, Inaba M, Kumeda Y, Hiura Y, Shirakawa K, Yamada S, Henmi Y, Ishimura E, Nishizawa Y (2006) Increased pulse wave velocity in subclinical hypothyroidism. J Clin Endocrinol Metab 91:154–158. doi:10.1210/jc.2005-1342

Naylor C (1994) The rational clinical examination: physical examination of the liver. JAMA 271:1859–1865. doi:10.1001/jama.271.23.1859

Ophir J, Cespedes I, Ponnekanti H, Yazdi Y, Li X (1991) Elastography—a quantitative method for imaging the elasticity of biological tissues. Ultrason Imaging 13:111–134. doi:10.1016/0161-7346(91)90079-W

Phipps S, Yang T, Habib F, Reuben R, McNeill S (2005) Measurement of tissue mechanical characteristics to distinguish between benign and malignant prostatic disease. Urology 66:447–450

Provenzano PP, Inman DR, Eliceiri KW, Knittel JG, Yan L, Rueden CT, White JG, Keely PJ (2008) Collagen density promotes mammary tumor initiation and progression. BMC Med 6:11

Sandrin L, Fourquet B, Hasquenoph J, Yon S, Fournier C, Mal F, Christidis C, Ziol M, Poulet B, Kazemi F, Beaugrand M, Palau R (2003) Transient elastography: a new noninvasive method for assessment of hepatic fibrosis. Ultrasound Med Biol 29:1705–1713. doi:10.1016/j.ultrasmedbio.2003.07.001

Shefelbine SJ, Simon U, Claes L, Gold A, Gabet Y, Bab I, Muller R, Augat P (2005) Prediction of fracture callus mechanical properties using micro-ct images and voxel-based finite element analysis. Bone 36:480–488. doi:10.1016/j.bone.2004.11.007

Sinkus R, Tanter M, Bercoff J, Siegmann K, Pernot M, Athanasiou A, Fink M (2008) Potential of mri and ultrasound radiation force in elastography: applications to diagnosis and therapy. Proc IEEE 96:490–499. doi:10.1109/JPROC.2007.913536

Souchon R, Rouviere O, Gelet A, Detti V, Srinivasan S, Ophir J, Chapelon J-Y (2003) Visualization of hifu lesions using elastography of the human prostate in vivo: preliminary results. Ultrasound Med Biol 29:1007–1015. doi:10.1016/S0301-5629(03)00065-6

Sullivan JM, Charron G, Paulsen KD (1997) A three-dimensional mesh generator for arbitrary multiple material domains. Finite Elem Anal Des 25:219–241. doi:10.1016/S0168-874X(96)00027-3

Tilleman TR, Tilleman MM, Neumann MHA (2004) The elastic properties of cancerous skin: Poisson's ratio and young's modulus. Isr Med Assoc J 6:753–755

vanPopele NM, Grobbee DE, Bots ML, Asmar R, Topouchian J, Reneman RS, Hoeks APG, vanderKuip DAM, Hofman A, Witteman JCM (2001) Association between arterial stiffness and atherosclerosis: the rotterdam study. Stroke 32:454–460

Venkatesh SK, Yin M, Glockner JF, Takahashi N, Araoz PA, Talwalkar JA, Ehman RL (2008) Mr elastography of liver tumors: preliminary results. Am J Roentgenol 190:1534–1540

Yeh WC, Li PC, Jeng YM, Hsu HC, Kuo PL, Li ML, Yang PM, Lee PH (2002) Elastic modulus measurements of human liver and correlation with pathology. Ultrasound Med Biol 28:467–474

Ziol M, Handra-Luca A, Kettaneh A, Christidis C, Mal F, Kazemi F, de Ledinghen V, Marcellin P, Dhumeaux D, Trinchet JC, Beaugrand M (2005) Noninvasive assessment of liver fibrosis by measurement of stiffness in patients with chronic hepatitis c. Hepatology 41:48–54